
SPE 99351

# Case Studies: A Practical Approach to Gas-Production Analysis and Forecasting

C.L. Jordan, M.J. Fenniak, and C.R. Smith, Rapid Technology Corp.



This paper was prepared for presentation at the 2006 SPE Gas Technology Symposium held in Calgary, Alberta, Canada, 15–17 May 2006.



## Abstract

This paper illustrates a practical systematic approach to determine the reservoir flow characteristics and reserves for both conventional and unconventional gas wells. Currently, there is an industry assortment of production analysis methods ranging from exponential decline and typecurve matching to rate-pressure normalization techniques and detailed production history matching. Through real life cases studies it will be shown that it is possible that a simpler reservoir model, such as a single well completed in the center of a circular reservoir, could be used to represent far more complex reservoirs, and still provide some representative reservoir characterization, as well as accurate reserves analysis and production forecasting. As a result, it possible that engineers and the like can avoid some of the more labor intensive production data analysis (PDA) techniques, and use more a methodology similar in operation to traditional decline.

Case studies and experience presented in this paper will demonstrate that a simple approach of production analysis methods will allow for a) proper identification of flow regimes, b) reliable evaluation of drainage area and OGIP, and c) the prediction of future deliverability and depletion. Case studies will also show that up-scaled and aggregate reservoir properties can provide a real measure of gas well deliverability (therefore a simpler, time-efficient model analysis can be used). Data uncertainty, unconventional gas (i.e. coal bed methane, tight gas, shale gas), stimulation appraisal, and other factors will be discussed in the context of the case studies.

## Introduction

The most common reason for analyzing gas production data is to estimate reserves and future production of gas wells. In forecasting, a variety of methodologies exist ranging from simple decline to complex numerical simulation. In many instances, even pressure transient analysis (PTA) is used to form the basis of a forecast model. However, usually due to time limitations, only empirical methods such volumetrics, and conventional decline analysis are used. As a result, there is challenge is to get the most out of information embedded in production and flowing pressure data to provide improved mechanistic predictions of future gas well performance.

Again, sophisticated methods, such as numerical simulation, have been available for decades and may provide the answers that industry needs. Although their predictive capabilities are proven, the accessibility (i.e. ease of use) of these methods is the issue. Of course, if time permits, all other techniques should be used.

## Background

Early attempts to linearize and extrapolate production history were limited. Future production could be estimated if one assumed that the production trend remained linear and constant for the remaining life of the well (i.e. stable fluid properties, constant flowing bottom-hole pressure (BHP) etc.). The difficulty of applying this type of decline analysis for gas cases is that these assumptions are severely restrictive and are therefore frequently violated. Again, given business time constraints, the aforementioned methods are the norm for industry.

In order to address the deficiency of standard decline analysis, typecurve analysis has been developed over many years. Typecurves are plots of theoretical solutions to flow equations (usually constant flow rate, or constant BHP) and can be generated for any kind of reservoir model for which a solution describing the flow behavior is available. Typecurve analysis theoretically allows one to estimate gas-in-place and gas reserves at some abandonment condition, as well as flowing characteristics of individual wells (i.e. permeability and skin). A common set of decline typecurves are those presented by Fetkovich (1980). Although more reservoir information is learned using Fetkovitch typecurves, they were still limited by the assumption of constant BHP, and constant fluid properties. Carter (1985) offered improved accuracy by using a plotting function that included the changes in fluid properties with average pressure. These curves were still limited to the assumption of constant flowing pressure. Carter's approach was similar to the pseudo-time function introduced by Agarwal (1979) in which the focus was to account for pressure dependant fluid properties in the near wellbore region during a flow and buildup analysis. Fraim and Wattenbarger (1987) also introduced a pseudo-time function to transfer a gas system into a single phase liquid system.

In order to alleviate the problem that many typecurves were limited to an assumption of constant flowing pressure,

Blasingame and Lee (1986) introduced a plotting variable called "material balance time" which allowed an equivalent constant rate solution to be extracted from a variable rate history. This equivalent solution was then applied to typecurve analysis, also accounting for pressure dependant properties via pseudo-time based on average reservoir pressure. Other methods of extracting a constant rate or constant pressure response from variable rate-pressure data include deconvolution schemes such as those proposed by Bostic, Agarwal, and Carter (1980), or Kucuk and Ayestaran (1985). These days, there are a growing number of typecurves available, including: hydraulically fractured wells in bounded reservoirs, composite reservoir scenarios, horizontal wells and more.

## Proposal: Equivalent Radial Homogeneous Models

It is proposed that a simpler reservoir model (a single well completed in the center of a circular reservoir) can be used to represent a far more complex reservoir system and still provide some representative reservoir characterization and accurate production forecasting. Jordan, Fenniak, and Sibbald[1] empirically showed (using synthetically generated data) that radially composite reservoirs, dual porosity reservoirs, etc. could be effectively reduced to an "equivalent radial homogeneous" (ERH) model with accurate reserves, and a gross effective permeability. Most of the work by Jordan[1] *et al* was based on introducing permeability calculations into the popular a) "rate-cumulative production typecurves" introduced by Argawal[2] *et al* and Gardner[3] *et al*, as well as b) "normalized rate-time plots" introduced by Wattenbarger[5,6,7] *et al*. The objective of these authors was to find a method evaluating OGIP, based solely on production data, without considering reservoir flow capacity etc. Another inspiration was Toh[4] who demonstrated, using extensive numerical simulation, that random permeability fields and somewhat sectionally homogeneous reservoirs could be represented by an average effective permeability during pseudo-steady state (PSS) flow – his work focused solely on calculating equivalent effective permeability from decline equations for oil and gas.

Termed as "Normalized decline" in this paper, the aforementioned methods by Argawal[2] *et al*, Wattenbarger[5,6,7] *et al*, and others seek to linearize variable rate-pressure to equivalent single rate or constant pressure cases for OGIP. With a slight modification of the normalized decline plots, equivalent permeability can also be extracted as suggested by Toh[4]. A review of Appendix 1 will show a derivation of Normalized Rate vs. Cumulative Production analysis (or NRQ analysis) whereby OGIP is determined from the x-intercept of the normalized data, and permeability is extracted from the y-intercept. A review of Appendix 2 will show a derivation of Normalized Rate vs. Time (or NRT analysis) whereby OGIP is determined from the slope of the linearized data, and permeability is also extracted from the y-intercept. Both of these relations are derived from the classic PSS flow equation[8].

A review of the final solution for each normalization technique will show that the y-intercept is proportional to permeability, drainage area, net pay, and even shape factor. Initially, this might be intimidating as it implies that permeability can only be accurately determined if all these other factors are shown. However, since the y-intercept in each linearization method is a single term, then the effective permeability will compensate for errors in the other parameters. In other words, if a shape factor, net pay, and skin are assumed for a given data set, there is an ERH model that represents the original reservoir on a PSS basis.

Now, it is understood that these linearization methods were developed under the assumption that PSS flow exists. Specifically, permeability, wellbore skin, net pay, etc. are not so interchangeable during transient flow periods. However, long-term deliverability and productivity is generally of more concern than transient or flush production.

Nonetheless, it may be argued that these simple linearization techniques may only be applicable to conventional gas reservoirs, and that an ERH model may not be suitable to coal gas, tight gas, shale gas or other unconventional scenarios such as stress dependant permeability and porosity. The motivation behind this paper was to investigate a variety of well documented data sets (both field and simulated) which fall under the umbrella of unconventional gas, and determine the applicability of an ERH model by evaluating reserves estimation, production forecasts, typecurves, and even stimulation effectiveness. In all cases, a shape factor ($C_A$) of 31.62 was used, implying a well completed in the center of a circular reservoir[9]. Also, a wellbore skin of "0" was assumed unless otherwise stated.

## Case Studies

**Case 1: Internal Boundary.** This model consisted of a vertical well completed in the center a circular drainage area (Figure 1), and was heavily studied by Sageev *et al*[9]. Offset from the well is a large circular zero permeability region, or internal boundary. In this case, a large 72 Acre internal boundary was placed 100 ft away from the well (with a center-to-center distance of 1100 ft). Reservoir permeability was set to 20 md. Overall pool area (including the internal boundary) was 640 Acres. The net OGIP, excluding the pay associated with the internal boundary, was 5.4 Bcf. These parameters are summarized in Table 1. All of the work presented by Sageev *et al*[9] was synthetic.

The NRQ and NRT analysis (Figures 2 and 3), based on 1 year data, indicated an average reservoir permeability of 16 md and OGIP of 5.4 Bcf. The corresponding net drainage area was calculated to be 568 acres, a difference of 72 acres from the gross pool boundaries. Since a shape factor ($C_A$) of 31.62 was used in the analysis, it is expected that permeability would be calculated incorrectly – basically, the permeability compensated for the error in shape factor.

Next, based on the normalized decline results, 5 year forecasts (Figure 4) were generated using the simple radial model presented by van Everdingen and Hurst[10]. A review of this plot shows that the normalized decline analysis produced an ERH model which could be used accurately for estimating reserves and generating extended production forecasts. This is an important illustration that the complexity of permeability variations in reservoirs need not necessarily be fully described in order for a reliable forecast to be made.

Figure 5 shows the dimensionless constant rate typecurves (CRT) for both the internal boundary model and the simplified ERH model. It is obvious that the ERH model does not accurately characterize the transient behavior of this data. The effect of the large low permeability area on variations in the derivative trend is clearly seen for the Sageev *et al*[9] et al model. However, if only monthly data was used in the analysis, then we find that the raw data generally only really reflects PSS (Figures 6 and 7 show the Bourdet[11] and Blasingame[12] *et al* typecurves respectively).

**Case 2: Tight Gas Well C231.** Recently, Arevalo-Villagran[13] *et al* published a methodology whose objective was to present physical scenarios that cause long-term linear flow in tight gas reservoirs (i.e. linear flow during both transient boundary dominated flow regimes), and then characterize these reservoirs using specialized diagnostic plots (i.e. $\Delta m(p)/q_g$ vs. $t^{0.5}$, and vs. $\Delta m(p)/q_g$ vs. $t^{0.25}$). Some of the results that were found were that long-term flow in tight gas wells may be developed and controlled because of the presence of natural fracturing in the reservoirs, or natural paths and streaks of higher permeability/conductivity. Other possible conclusions were that hydraulic fractures may extend to the drainage boundary[14].

Six of the wells (known as the Castlegate tight gas wells) analyzed were located in Utah, U.S.A. One particular well, C231, was analyzed in this paper (Figure 8 shows the raw data). Initially, these wells data were plotted on a $\Delta m(p)/q_g$ vs. log (t) plot to identify radial flow. A "semi-log straight line" was found for each well and "k" and "s" were calculated, using the perforated interval as "h" (refer to Figure 9). The calculated permeability and skin for C231 was 0.04 md and -4.79, respectively. Next, using a plot of $\Delta m(p)/q_g$ vs. (t), OGIP was calculated to be 0.9 - 1.0 Bcf, with a drainage area of 51 to 54 Acres, and a shape factor of 0.68 (refer to Figure 10). The parameters for wells are summarized in Table 1. Incidentally, the PSS superposition time function used by the authors of the original work could have been replaced by Material Balance Time[3,6,7]. Results were later verified using the well known Gassim Simulator[15].

Using the normalized decline method (refer to Figures 11 and 12) and ERH methodology, the OGIP was determined to be 0.7 Bcf with an average effective permeability of 0.17 md (again, the permeability calculation was of course based upon an assumed shape factor of 31.62 and an assumed skin of 0). Drainage area was estimated to be 35 Acres. As a further experiment, the same data was re-analyzed assuming a skin -4.79 (refer to (7) in Appendix 1): the resulting permeability was calculated to be 0.054 md, while Area and OGIP remained at 35 Acres and 0.7 Bcf, respectively. Production forecasts were then generated using both ERH models, and the results were found to be identical confirming the hypothesis that equivalent radial models exist that would suitably predict long-term deliverability. Figure 8 shows both ERH models, as well as the original data set. Of course, transient behavior would be different for both models.

**Case 3: Stress Dependant Permeability.** In 2004, Rodriquez[18] performed an extensive investigation into the pressure and production performance on tight gas reservoirs with considerations for stress dependant permeability during transient and PSS. In his work, permeability was assumed to vary exponentially with both pore pressure (refer to (12) in Appendix 3) and permeability modulus ($\gamma$) (as defined by Nur *et al* [19]). For his purposes, Rodriquez[18] limited the permeability modulus to a range of 0.0 to 0.001, with 0.001 having the most impact on permeability as reservoir depletion occurred. Also, Rodriquez's work focused solely on simulated data, as opposed to field measured rates and pressures.

Although Rodriquez evaluated varying level's of pressure dependency, he limited his bounded radial reservoir models to the following parameters: a drainage radius of 3,000 ft, an OGIP of 259 Bcf, and a base permeability of $2.5 \times 10^{-3}$ md. These parameters are summarized in Table 1. Production rates were set to constants, but he did vary the constant rate from case to case. Constant rate simulation runs were also performed using the Gassim Simulator[15] . Flowing sandface pressures were calculated, and then compared.

For the purposes of this paper, Rodriquez's data for $\gamma = 0.0008$ was examined using the normalized decline and ERH methods. Using Rodriquez's data for a constant production rate of $q_g$ of 10 mscf/d, normalized decline (Figure 13) indicated a drainage radius of 2,648 ft, an OGIP of approximately 202 Bcf, and an effective permeability of $2.1 \times 10^{-3}$ md. Figures 14, 15, and 16 showed reasonable matches between the ERH and the raw data. The figures also showed the majority of data falls on PSS making transient analysis redundant. Initially it was thought that that the error in OGIP was within reason, but a review of the work provided by Rodriquez will provide a correlation that showed calculated OGIP would be pessimistic if pressure dependency was not taken into account. A review of Figure 17, which shows two cases with different constant flow rates, demonstrates error introduced by the impact of pressure dependency amplifies with greater rates of depletion. Nonetheless, the error did initially appear to be acceptable, the calculated reservoir parameters suitable, and the normalized decline and ERH methods successful.

As a further test, another of Rodriquez's cases was analyzed using the normalized decline and ERH approach. All parameters were the same as before except that the drawdown rate was 20 mscf/d as opposed to 10 mscf/d. Results indicated a significantly lower OGIP of 131 Bcf – this error could not be attributed to anything other than the methodology. It was believed that the normalization procedure was not applicable to reservoirs with pressure dependant rock properties such as porosity and/or permeability. However, if the normalized equations are rederived in the same manner as presented in Appendices 1 and 2, except that $k = k_a k(P_R)$, then we find that the data can again be normalized such that the correct OGIP and base (or initial) permeability are determined. Of course, we imply "correct" permeability based on a shape factor 31.62. Appendix 3 shows the new formulation of the normalized equations. In each case, the y-intercept returns the base or initial permeability. A review of Figure 18 will show that NRQ analysis now provides a correct estimate of OGIP.

We believe, as long as non-linear permeability was taken into account, the normalized decline method would determine the correct reserves.

**Case 4: Tight Gas Well J7**. Wattenbarger, El-Banbi, and Maggard presented an analysis of tight gas wells from a field in South Texas, one of which was J7. The well was hydraulically fractured and had been producing for nearly 23 years. Monthly production rates and fluid/rock properties are the only data available. Refer to Table 1 for the listing of the reservoir parameters for this well.

After a number of simulation runs and regressing on model parameters, the two best fits reported by the authors were that of the linear homogeneous closed reservoir and radial transient dual porosity closed reservoir providing an OGIP ranging from 6.9 – 7.1 Bcf. Two other models (linear PSS dual porosity closed reservoir and linear transient dual porosity closed reservoir) did not provide a suitable match. Incidentally, the operator and others believed that the field had some natural fractures in one direction and that these natural fractures enhanced the permeability in their direction resulting in anisotropic behavior (for such a reservoir shape, linear flow was anticipated to be observed for majority of the life of the well).

Normalized decline analysis (Figure 19) provided an initial OGIP of 4.9 Bcf (which is slightly lower than the reported results), with an effective permeability of 0.01 md, and a drainage area of 49 Acres. A review of the production history match indicated that the results were generally suitable (Figure 20). A review of the dimensionless constant rate and constant pressure typecurves did not provide any further insight. Incidentally, the majority of the "interpretable" data fell onto the PSS portion of the curve.

We believe the normalized decline method can determine correct reserves and effective permeability in tight gas situations.

**Case 5: Tight Gas Wells HR-58 / HR-60**. Wells HR-58 and HR-60 are in high pressure, tight gas reservoirs were the subject of analysis by Ibrahim [5,6,7]. The data for both wells are given Table 1. In the original work, Ibrahim focused on the original form of the normalization technique presented in Appendix 2. Those results indicated the OGIP for HR-58 and HR-60 to be 9.8 and 7.15 Bcf respectively. The OGIP values were estimated using a linearization procedure in which $\Delta m(p)/q_g$ was plotted as against super-$t_{a,pss}$ (superposition PSS pseudotime). The aforementioned analysis was comparable to the work done by Arevalo-Villagran[13] *et al.* Permeability was estimated, presumably through simulation and pressure transient analysis, to be 0.038 md and 0.06 md, respectively. Incidentally, the objective of the original work was to illustrate the impact of pressure dependant gas properties on reserve estimation in the linearization process.

Using the normalized decline procedure outlined by the authors of this paper, OGIP for HR-58 and HR-60 wells were estimated to be 7.7 and 6.6 Bcf respectively. The corresponding permeabilities were found to be 0.14 and 0.22 md. The differences in calculated permeability may have been due to stimulated conditions of the wells (which was not reported), or shape factor.

As a further experiment, both wells were re-analyzed using ¼ of the net pay reported. As expected, normalized decline resulted in the same OGIP, but the calculated permeabilities for HR-58 and HR-60 were now calculated to be 0.62 and 1.0 md respectively. Figures 21 and 22 show the NRQ for these wells while Figures 23 and 24 show the production history matches using the ERH models based varying net pay. As can be seen, regardless of the net pay and permeability combination, suitable production models can be generated. Assuming the incorrect net pay may be compensated by changes in permeability (in a manner similar to skin), but the resulting drainage area would be incorrect, and may have an impact of drilling density. Due to noise and data scatter, the Bourdet[11], Blasingame[12], and even the NPI[20] typecurves did not provide more insight than verification of PSS and reserves.

**Case 6: Dry Coal Gas**: In this section, the normalized decline and ERH methodology is applied to numerically generated single phase CBM production data (as presented by CBM pioneers Clarkson and McGovern[18]). In their original work, Clarkson and McGovern, using the Eclipse™ numerical simulator, evaluated the accuracy of tank models for 2 phase and single phase CBM production matching and forecasting. For their single phase applications, they assumed a single well centrally located within a bounded reservoir with a drainage area of 160 Acres. Based on the specified Langmuir volume (250 scf/ton, in-situ) and Langmuir pressure (661 psia), the OGIP was calculated to be 1.6 Bcf at an inital reservoir pressure of 600. A listing of the remaining reservoir parameters are given in Table 1.

However, prior to performing the normalized decline analysis, it was anticipated that the material balance calculations for pseudo-time and average reservoir pressure would have to be altered to account for the additional gas adsorbed on the coal surface. This was done using the modified "P/z" calculation introduced by King, who presented material balance techniques for Coal-Seam and Devonian Shale Gas Reservoirs with Limited Water Influx[19]. It is important to note that other authors have presented suitable material balance techniques for single and two-phase coal, and that King's approach was chosen arbitrarily.

Accounting for the effect of coal compressibility (i.e. coal gas content) within the material balance and pseudo-time calculations, we find that the normalized decline approach will also linearize CBM data (Figures 25 and 26), in a manner identical to conventional gas. As a result, absolute effective permeability and OGIP can be derived from either of the normalized decline plots. A production match of the original simulated data and ERH model are shown in Figure 27. Plots of the Blasingame[12], NPI[20], and Bourdet[11] typecurves are shown in Figures 28, 29, and 30, indicate that the linearization procedure and ERH model both work well. The Bourdet typecurve shows significant scatter, making transient interpretation difficult. It is not believed that the original simulations run by Clarkson and McGovern made use of matrix shrinkage effects sometimes observed in coals. However, given the observations from the Case 3, it is anticipated that non-linear pressure and porosity behavior in coal seams could be incorporated into the normalized decline methodology. Authors such as Somerton[21] *et al* proposed a

correlation that allows formation permeability to vary with the changes in net stress $\Delta\sigma$, which can be correlated to changes in pore pressure $\Delta\sigma = 0.572\ \Delta p$ as suggested by Walsh[22]. Appendix 4 proposes a method to adapt the normalized decline method to two-phase coal. Although not presented, the authors have tested this extensively.

As a further test of the normalized decline / ERH methodology and its applicability to reservoirs that obey isotherms, production data from the Barnett Shale was also evaluated; in particular, data taken from the Stella Young Well presented by the GRI in 1991[23]. Although not presented in this paper, similar success was observed.

**Case 7: Hydraulic Frac / Tight Gas Well**. In the work by Baree[24] *et al*, Well #1 (as denoted in the original work) was a stimulated well. OGIP and drainage area was estimated using the matching technique based upon the work of Agarwal and Gardner[2] (Figure 34). Once the effective drainage area was determined, reservoir flow capacity and effective fracture half-length was derived from a semi-log plot of normalized pressure versus adjusted time. Results from the original work indicated a finite conductivity fracture in square reservoir with a flow capacity of 3.27 md-ft, with a reservoir permeability of 0.14 md. Fracture half-length was calculated to be 22 ft from production modeling, and 369 ft from pressure buildup analysis.

Again using the normalized decline approach outlined in this paper, the raw data was analyzed for OGIP and average effective permeability. Assuming a circular reservoir with a well located in the center, the area was calculated to be 136 Acres, the OGIP 2.1 Bcf, with an average effective permeability of 0.28 md. The NRQ is shown in Figure 32.

Although the calculated permeabilities differ by a factor of 2, both models provide a suitable production match for the raw data during stabilized production (and even transient flow). Figure 31 shows a comparison of the original raw data and model provided by Baree *et al*, as well as the model by the authors of this work. The differences between the raw data and models is nearly imperceptible. The typecurve match from Baree[24] *et al* is shown in Figure 33, while the Bourdet[11], Blasingame[12], and even the NPI[20] are shown in Figures 35, 36, and 37 respectively. These typecurves suggest that the pressure data could be modeled with a radial homogenous reservoir, as opposed to a infinite-conductivity fracture model.

## Conclusions & Future Work

After completing and reviewing the above case studies (as well as related work), it was concluded that:

a) Complex and heterogeneous reservoirs can be reduced to simpler, equivalent radial homogeneous (ERH) reservoirs during pseudo-steady state. Specifically, it has been observed that these reservoirs deplete like homogeneous reservoirs.
b) The effective permeability of these ERH models compensates for errors in shape, heterogeneity, near wellbore formation damage, and even net pay.
c) If OGIP is honored correctly, then accurate production forecasts can be generated using the ERH model, assuming the equivalent effective permeability is used. Non-linear transformations such as pseudo-pressure and pseudo-time should also be honored.
d) These ERH models can be applied to conventional and unconventional gas including tight gas, single-phase and two-phase coal gas, and even shale gas, as long as consideration is given to any non-linear behavior in the linearization process.
e) However, despite the success thus far, further work should be done to evaluate other non-conventional gas and heterogeneous systems. Toh[4], for example, suggested that sectionally homogenous with extremely large permeability contrasts may not entirely be amendable to ERH.

## Nomenclature

| | |
|---|---|
| $A$ | Reservoir Area, $ft^2$ |
| $B_{gi}$ | Gas FVF at Initial Conditions (Dim) |
| $C_A$ | Shape Factor, Dimensionless |
| $c_t$ | Total System Compressibility ($psia^{-1}$) |
| $c_{ti}$ | Total System Compressibiity at $P_i$ ($psia^{-1}$) |
| $h$ | Net pay (ft) |
| OGIP | Original-Gas-In-Place (scf) |
| $m(p)$ | Pseudo-pressure of "P" ($psia^2/cp$) |
| $m(p_i)$ | Pseudo-pressure of "$P_i$" ($psia^2/cp$) |
| $n$ | Index |
| $P$ | Pressure (psia) |
| $P_i$ | Initial Reservoir Pressure (psia) |
| $P_{wf}$ | Flowing Sandface Pressure (psia) |
| $P_R$ | Average Reservoir Pressure (psia) |
| $p_D$ | Dimensionless Pressure |
| $q_g$ | Gas Rate at Standard Conditions (mscf/d) |
| $Q_g$ | Cumulative Gas Produced |
| $S_{wi}$ | Initial Water Saturation (fraction) |
| $s'$ | Wellbore skin |
| $t$ | Time (hrs) |
| $t_a$ | Pseudo-time (hrs) |
| $t_D$ | Dimensionless Time referenced to $r_w$ |
| $t_{Da}$ | Dimensionless Pseudo-Time referenced to $r_w$ |
| $t_{DA}$ | Dimensionless Time referenced to Area (A) |
| $k$ | Permeability (md) |
| $r_w$ | Wellbore radius (ft) |
| $r_{wa}$ | Apparent Wellbore Radius (ft) |
| $T_f$ | Formation Temperature ($^oR$) |
| $\gamma$ | Euler's Constant |
| $\gamma_m$ | Permeability Modulus |
| $\phi$ | Porosity |
| $\mu$ | Gas viscosity (cp) |
| $\sigma$ | Stress |
| $z_i$ | Gas deviation factor |

### Subscripts:

| | |
|---|---|
| a | Pseudo-time |
| A | Area |
| D | Dimensionless |
| g | Gas |
| i | Initial |
| PSS | Pseudo-steady state |
| t | Total |

wf Wellbore Flowing
w Wellbore
m Modulus

## References:


1. JORDAN, C.L., FENNIAK, M., SIBBALD, L.R., "Simple Accurate Gas Production Analysis for Forecasting & Reserves", CIPC June 7-9, 2005, Calgary, Alberta.
2. AGARWAL, R.A., GARNDER, D.C, AND KLEINSTEIBER, S.W, "Analyzing Well Production Dada Using Combined-Type-Curve and Decline Curve Analysis Concepts", SPE 57916, 1988 SPE Annual Technical Conference and Exhibition, New Orleans, Louisiana
3. GARDNER, D.C., HAGER, C.J., AND ARGARWAL, R.G., "Incorporating Rate-Time Superposition into Decline Type Curve Analysis", SPE Paper No. 62475 prepared for presentation at the 2000 SPE Rocky Mountain Regional Meeting/ Low Permeability Reservoirs Symposium, Denver, 12-15 March.
4. TOH, S.K., "The Depletion Performance of Heterogeneous Reservoirs", Ph.D Thesis, Texas A&M, 1997.
5. IBRAHIM, M.H. "History Matching Pressure Response Functions From Production Data", Ph.D Thesis, December 2004, Texas A&M Univeristy.
6. IBRAHIM, M, WATTENBARGER, R.A., & HELMY, W. "Determination of OGIP for Tight Gas Wells – New Methods", CIPC 2003, Calgary, Alberta, CIPC Paper No. 2003-12.
7. IBRAHIM, M, WATTENBARGEr, R.A., & Helmy, W. "Determination of OGIP for Wells in Pseudosteady-State – Old Techniques, New Approaches", SPE ATCE, October 5-8th, 2003, Denver, Colorado, SPE Paper No. 84286
8. Gas Well Testing: Theory & Practice", 4th Ed. Metric. ALBERTA ENERGY & UTILITIES BOARD Publication.
9. BRITTO, P., and SAGEEV, A., "The Effects of Size, Shape, and Orientation of an Impermeable Region on Transient Pressure Testing", SPE California Regional Meeting, Ventura, April 8-10, 1987. SPE Paper No. 16376.
10. van EVERDINGEN, A.F., & HURST, W., "Application of the Laplace Transformation to Flow Problems in Reservoirs", *Trans*, AIME (1949), 186, 305-24.
11. BOURDET, D., AYOUB, J.A., and PICARD, Y.M., "Use of Pressure Derivative in Well Test Intepretation", SPE Formation Evaluation, June 1989.
12. PALACIO, J.C; and BLASINGAME, T.A.: "Decline Curve Analysis Using Type Curves Analysis of Gas Well Production Data," paper SPE 25909 presented at the 1993 Joint Rocky Mountain Regional and Low Permeability Reservoirs Symposium, Denver, 26-28 April.
13. AREVALO-VILLIGRAN, J.A., JORGE, A., GUTIERREZ-ACOSTA, T., and MARTINEX-ROMERO, N, "Analysis of Long-Term Behavoir in Tight Gas Reservoirs: Case Histories", SPE Latin American and Caribbean Petroleum Engineering Conference, Rio de Janeiro, Brazil, SPE Paper No 95117, June 20-23, 2005
14. WATTENBARGER, R.A., EL-BANBI, A., VILLEGAS, M.E., and MAGGARD, J.B., "Production Analysis of Linear Flow into Fractured Tight Gas Wells",SPE Rocky Mountain Reginoal/Low Permeability Reservoirs Symposium, Denver, Colorado, SPE Paper No. 39931, April 5-8, 1998.
15. LEE, A.J., and WATTENBARGER, R.A., "*Gas Reservior Engnieering*", SPE Textbook Series Vol. 5, SPE Richardson, TX (1996).
16. Rodriquez, C.A., "Stress-Dependent Permeability on Tight Gas Reservoirs", M.Sc. Thesis, Texas A&M University, December 2004.
17. Nur, A., and Yilmax, O., "Pore Pressure in Fronts in Fractured Rock Systems", Dept. of Geophysics, Stanford U., Stanford, CA (1985).
18. CLARKSON, C.,R., & McGOVERN, J.M., "A New Tool for Unconventional Reservoir Exploration and Development Applications", Internal Document, Burlington Resources Inc., Date Unknown.
19. KING, "Material Balance Techniques for Coal-Seam and Devonian Shale Gas Reservoirs with Limited Water Influx", SPE Reservoir Engineering, February 1993. SPE Paper No. 20730.
20. BLASINGAME, T.A., JOHNSTON, J.L., and LEE., W.J., "Type-Curve Analysis Using the Pressure Integral Method", SPE California Regional Meeting, Bakersfield, California, April 5-7, 1989. SPE No. 18799.
21. SOMERTON, D. et al "Effects of Stress on Permeability of Coal", Int. *J. Rock. Mech, Min. Sci. Geomech*. Abstr., **12**, 129-145.
22. WALSH, J. "Effect of Pore Pressure on Fracture Permeability", *Intl. J. Rock. Mech., Min Scin. Geomech*. Abstr., **18**, 429-435.
23. LANCASTER, D.E., and JOCHEN, J.E., "Analysis of Prodution and Well Test Data from Barnett Shale Wells Operated By Mitchell Energy Corporation", GRI Contract No. 5086-213-1446
24. BAREE, R.D., COX, S.A., GILBERT, J.V., and DOBSON, M., "Closing the Gap: Fracture Half-Length from Design, Buildup, and Production Analysis", SPE ATCE, Denver, Colorado, October 5- 8, 2003, SPE Paper No. 84491.
25. EARLOUGHER, Jr. R.C., "*Advances in Well Test Analysis*", SPE Monograph Series, Vol 5., SPE Dallas, TX (1977).
26. HURST., W. "Unsteady Fluid Flow in Oil Reservoirs", Physics 5, (January 1934), pg. 20-30.


## Appendix 1: Normalized "q" Vs. "Q"

The Normalized Rate versus Normalized Cumulative Production plot is based upon the work of Argawal *et al*[2]. In general, they showed that the linear relationship shown in (1) exists during PSS flow[10]. In the original work, OGIP was estimated by plotting the reciprocal of dimensionless wellbore pressure ($1/P_D$) versus cumulative production to generate a rate-cumulative-decline curve. This plot forms a straight line tending towards $1/(2\pi)$ during PSS, and is the basis of (1).

$$\frac{q_g}{m(p_i)-m(p_{wf})} \propto \frac{OGIP\left[m(p_i)-m\left(p_R(Q_g)\right)\right]}{m(p_i)-m(p_{wf})}+b \quad \text{.....(1)}$$

Originally (1) was derived for the purpose of determining original gas-in-place from flowing gas rate-pressure data. However, re-derivation of (1) from the common dimensionless PSS flow equation (2) shows that more than OGIP can be evaluated. Starting with (2), and substituting (3) which represent material balance gives (4) after substitution with standard dimensionless conversions. Appendix 5 outlines typical dimensionless variable definitions.

$$p_D = 2\pi \cdot t_{AD} + \frac{1}{2}\ln\left[\frac{4 \cdot A}{e^{\gamma} C_A r_{wa}{}^2}\right] \quad \text{.....(2)}$$

$$\overline{p_D} = 2\pi \cdot t_{AD} \quad \text{.....(3)}$$

$$\frac{(m(P_i) - m(P_{wf}))kh}{(1.417\times10^6)q_{sc}T_f} = \frac{(m(P_i) - m(P_R))kh}{(1.417\times10^6)q_{sc}T_f} + \frac{1}{2}\ln\left[\frac{4 \cdot A}{e^{\gamma} C_A r_{wa}{}^2}\right] \quad \text{.....(4)}$$

Now (4) can be altered further by taking the volumetric definition for OGIP (or G) shown in (5) and replacing net pay "h" in the first term to the right of the "equals" sign. As a result, the linear equation (6) is developed with (7), and (8) as defined.

$$\frac{B_{gi} OGIP}{h} = \phi A(1 - S_w) \quad \text{..... (5)}$$

$$\frac{q_g}{m(p_i) - m(p_{wf})} = -m\frac{OGIP\left[m(p_i) - m\left(p_R(Q_g)\right)\right]}{m(p_i) - m(p_{wf})} + b \quad \text{..... (6)}$$

$$b = \frac{kh}{(1.417\times10^6)T_f\left(\frac{1}{2}\ln\left[\frac{4 \cdot A}{e^{\gamma} C_A r_{wa}{}^2}\right]\right)} \quad \text{..... (7)}$$

$$m = \frac{k\frac{B_{gi}}{\phi A(1 - S_w)}}{(1.417\times10^6)T_f\left(\frac{1}{2}\ln\left[\frac{4 \cdot A}{e^{\gamma} C_A r_{wa}{}^2}\right]\right)} \quad \text{..... (8)}$$

Alternatively, (6) and (7) could have been derived from using the dimensionless equations first outlined by Argawal[2] *et al*. Also, (6) implies the use of pseudo-time and pseudo-pressure which account for some of the non-linear behavior of gas.

## Appendix 2: Normalized "q" Vs. "t"

The Normalized Rate versus Normalized time plot is based upon the work of Wattenbarger[6,7] *et al*. In general, they showed, they showed that the linear relationship (9) exists during PSS flow. It is apparent that (9) linearizes rate-time data where the OGIP is proportional to the slope as shown in (10). However, following re-derivation from (2) will show that "b", or the y-intercept is identical to the reciprocal of (7). Incidentally, the superposition PSS time function shown in (9) is identical to material balance time proposed by Blasingame *et al*. Also (9) incorporates both pseudo-time and pseudo-pressure to account for the pressure dependant properties of gas.

$$\frac{m(p_i) - m(p_{wf})}{q_{sc}} = m_{PSS}\left[\sum_{i=1}^{n}\frac{\Delta q_{sc,i}}{q_{sc,n}}(t_{an} - t_{ai-1})\right] + b \quad \text{..... (9)}$$

$$m_{PSS} = \frac{2P_i S_{gi}}{z_i(u_g c_t)_i}\left(\frac{1}{OGIP}\right) \quad \text{..... (10)}$$

## Appendix 3: Stress Dependant Permeability

The Normalized Rate versus Normalized time plot is based upon the work of Wattenbarger *et al*. In general, they showed, they showed that the following linear linear relationship exists during PSS flow:

$$k = k_i e^{-\gamma(P_i - P_R)} \quad \text{..... (11)}$$

$$\frac{\frac{q_g}{k(P_R)}}{m(p_i) - m(p_{wf})} = -m\frac{OGIP\left[m(p_i) - m\left(p_r(Q_g)\right)\right]}{m(p_i) - m(p_{wf})} + b \quad \text{..... (12)}$$

$$\frac{m(p_i) - m(p_{wf})}{\frac{q_g}{k(P_R)}} = m_{PSS}\left[\sum_{i=1}^{n}\frac{\Delta q_{sc,i}}{q_{sc,n}}(t_{an} - t_{ai-1})\right] + b \quad \text{.....(13)}$$

## Appendix 4: Other Non-Linear Permeability

Assuming PSS and material balance time, it is possible that (12) and (13) could be extended to other non-linear permeability scenarios such as two-phase CBM production. For example, if one recognizes $k_e = k_a k(S_w)$, where $S_w(P_R)$, then equations (12) and (13) hold for two phase production as well for permeability is ultimately a function of $P_R$ as originally shown for the pressure dependant permeability scenario. Evaluation of the "b" constants in both scenarios would return absolute permeability.

## Appendix 5: Dimensionless Variables

The following definitions for dimensionless variables are used throughout this paper.

$$p_D = \frac{kh\left(m(p_i) - m(p_{wf})\right)}{1.417 \cdot 10^6 T_f q_g} \quad \text{.....(14)}$$

$$\overline{p_D} = \frac{kh\left(m(p_i) - m(p_R)\right)}{1.417 \cdot 10^6 T_f q_g} \quad \text{.....(15)}$$

$$t_{AD} = \frac{0.0002637kt}{(\phi \mu_g c_t) A} \quad \text{.....(16)}$$

$$t_D = \frac{0.0002637kt}{(\phi \mu_g c_t) r_w^{\,2}} \quad \text{.....(17)}$$

$$t_{Da} = \frac{0.0002637kt_a}{(\phi \mu_g c_t) r_w^{\,2}} \quad \text{.....(18)}$$

Table 1: Case reservoir properties

| Case | Well | Net Pay (feet) | Porosity (%) | Pi (Psia) | k (md) | SG | $T_F$ ($^oF$) | OGIP (Bscf) | Sw (%) | Area (Acres) |
|---|---|---|---|---|---|---|---|---|---|---|
| Case 1 | Internal Boundary | 12.0 | 12.00 | 2500.00 | 20 | 0.65 | 120.0 | 5.4 | 20.00 | 640.0 |
| Case 2 | C231 | 30.0 | 9.00 | 6815.0 | 0.04 | 0.61 | 203.0 | 0.9-1.0 | 50.00 | 51.0-54.0 |
| Case 3 | Stress Dependant Perm. | 362.0 | 15.00 | 8800.0 | 0.00-0.001 | 0.717 | 290.0 | 259.0 | 47.0 | 649 |
| Case 4 | Well J7 | 92.0 | 15.00 | 8800.0 | 1.9 | 0.65 | 290.0 | 6.9 -7.1 | 47.0 | 68.0-78.9 |
| Case 5 | HR-58 | 374.5 | 13.54 | 14000.0 | 0.038 | 0.717 | 290.0 | 9.8 | 26.18 | N/A |
| Case 5 | HR-60 | 219.0 | 12.00 | 14000.0 | 0.06 | 0.717 | 290.0 | 6.6 | 23.5 | N/A |
| Case 6 | CBM | 40.0 | 0.30 | 600.0 | 0.5 | 0.544 | 100.0 | 1.60 | 0.0 | 160 |
| Case 7 | Well #1 | 24.0 | 11.00 | 3500.0 | 0.14 | 0.65 | 190.0 | 3.4 | 35.0 | 182 |

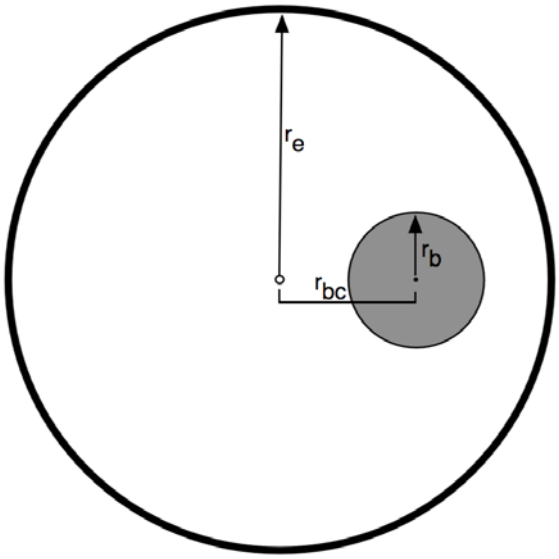


Figure 1: Internal Boundary Schematic

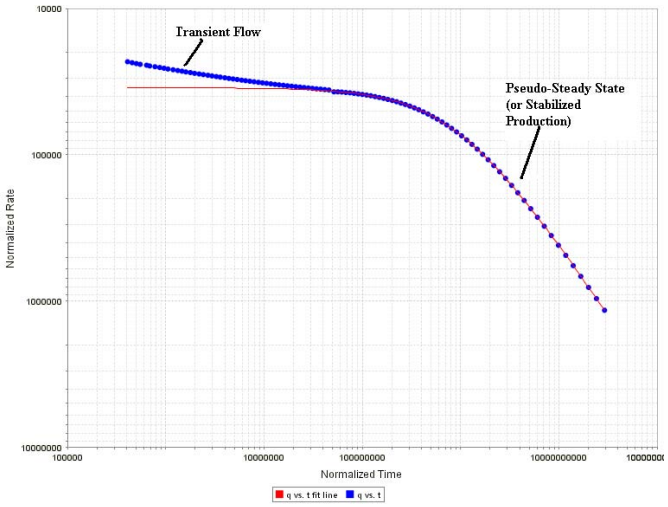


Figure 3: Normalized Rate vs. Normalized Time (Case 1)

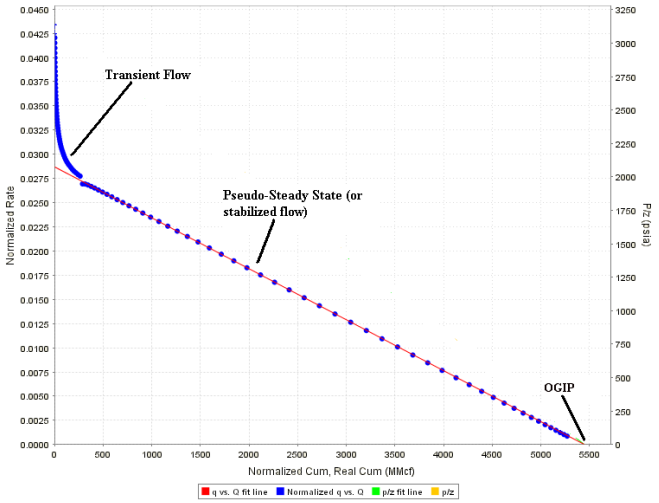


Figure 2: Normalized Rate vs. Cum. (Case 1)

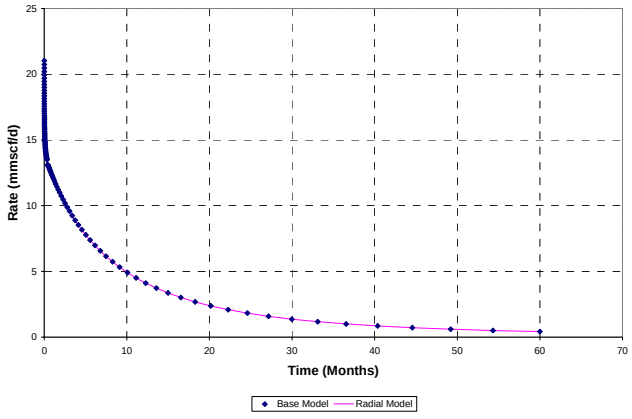


Figure 4: Five Year Forecast using Eqv. Radial and Internal Boundary Model

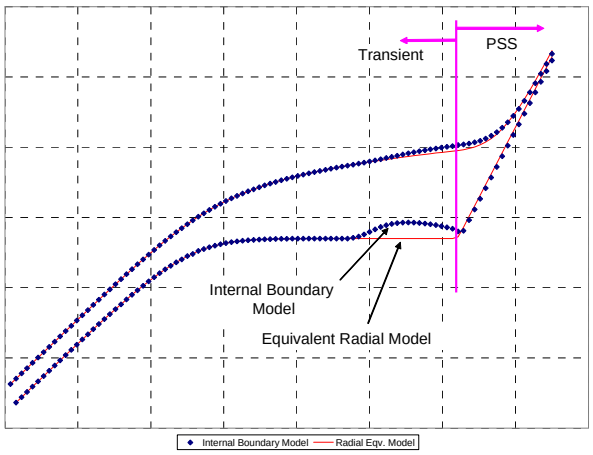


Figure 5: Contant Rate Typecurve – Internal Boundary (Case 1)

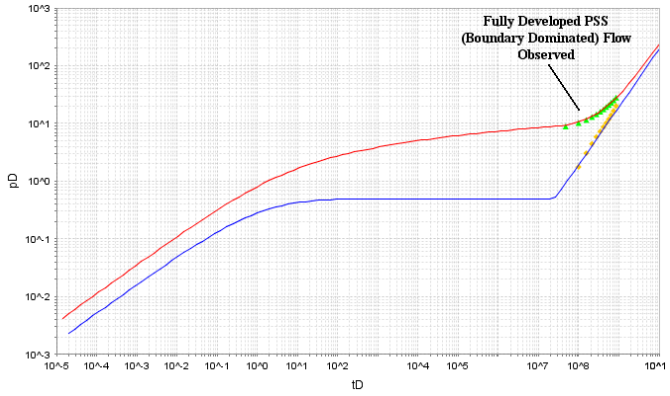


Figure 6: Constant Rate Typecurve for Internal Bounday Model (Case 1)

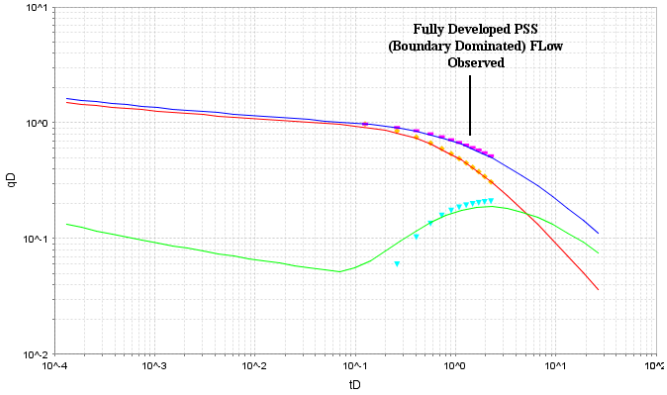


Figure 7: Constant Pressure Typecurve for Internal Boundary Model (Case 1)

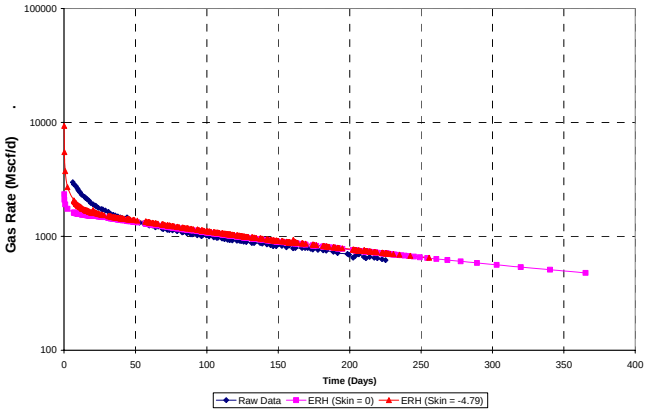


Figure 8: Raw Data and Models of Well C231 (Case 2)

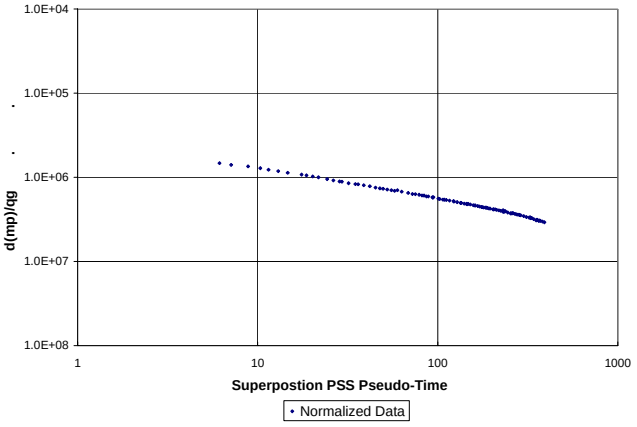


Figure 9: Semi-log straight line (Case 2)

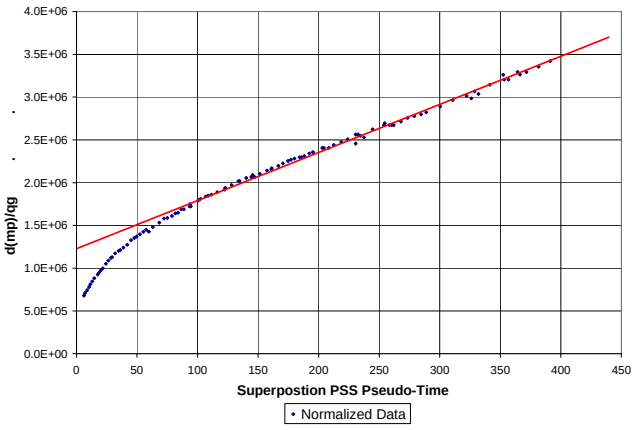


Figure 10: Normalized Rate vs. Time (Case 2)

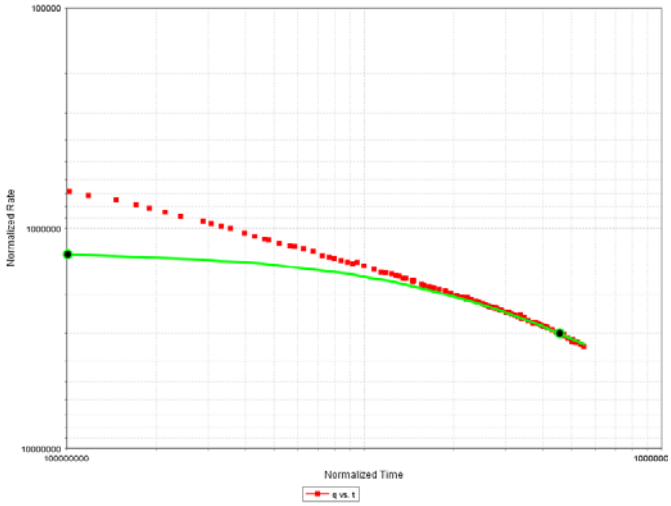


Figure 11: Normalized Rate vs Normalized Time (Case 2)

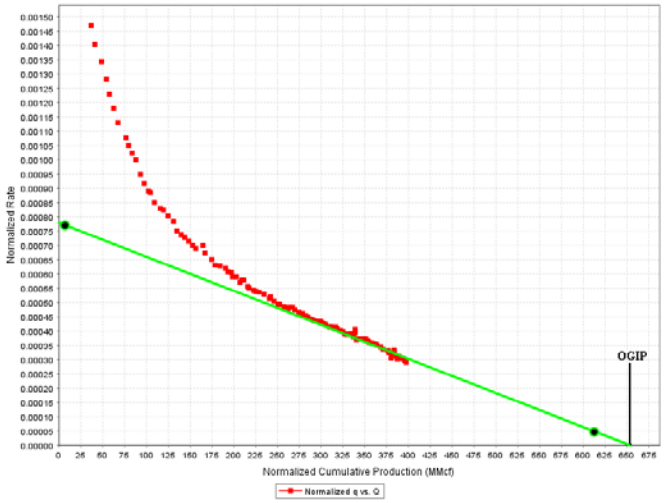


Figure 12: Normalize Rate vs. Normalized Cum. (Case 2)

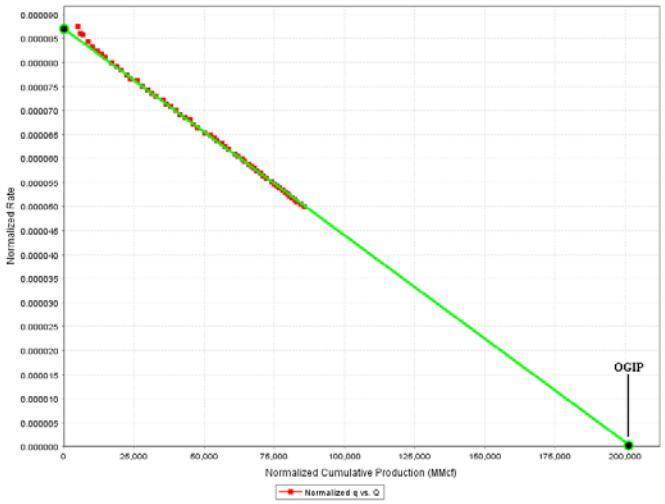


Figure 13: Normalized Rate vs. Normalized Cum. (Case 3)

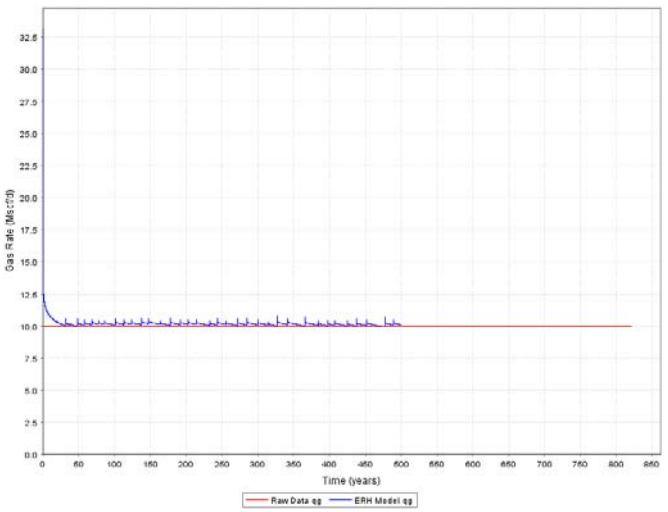


Figure 14: Production Data Analysis of Pressure Dependant Permeability (Case 3)

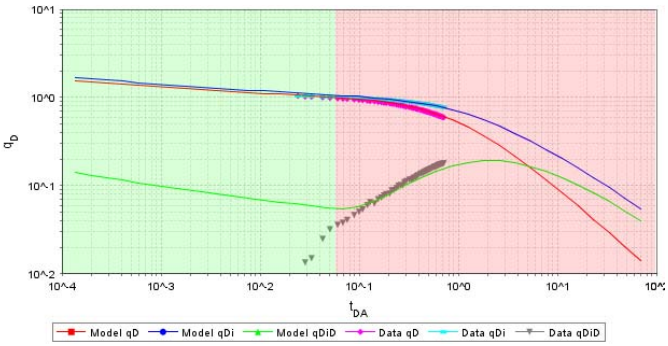


Figure 15: Blasigname Typecurve (Case 3)

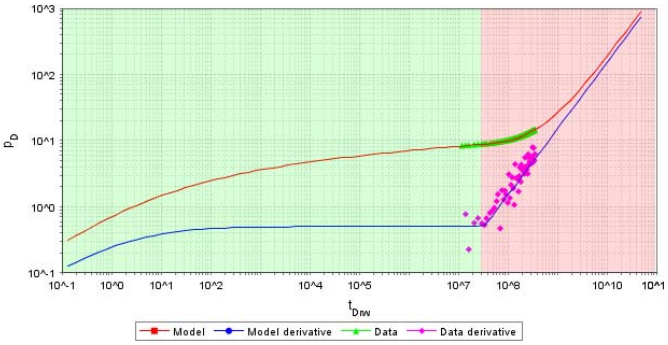


Figure 16: Bourdet Typecurve (Case 3)

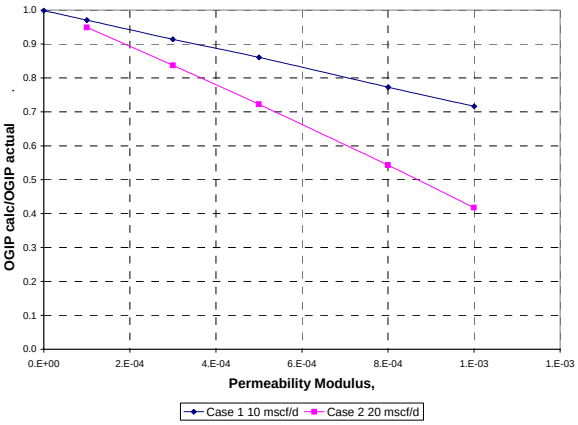


Figure 17: Stress Dependant Perm OGIP Calculation

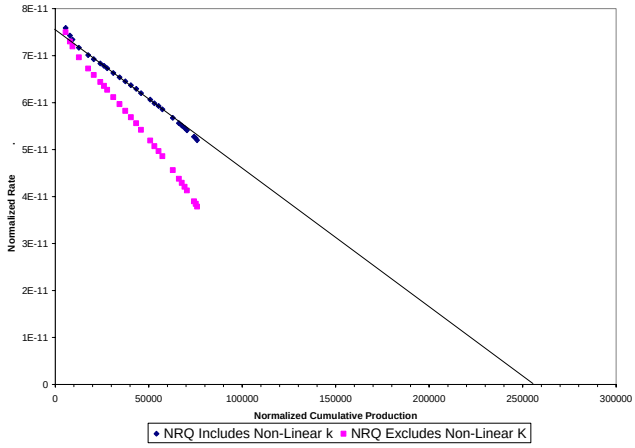


Figure 18: Raw Data vs. Normalized Decline (Case 3)

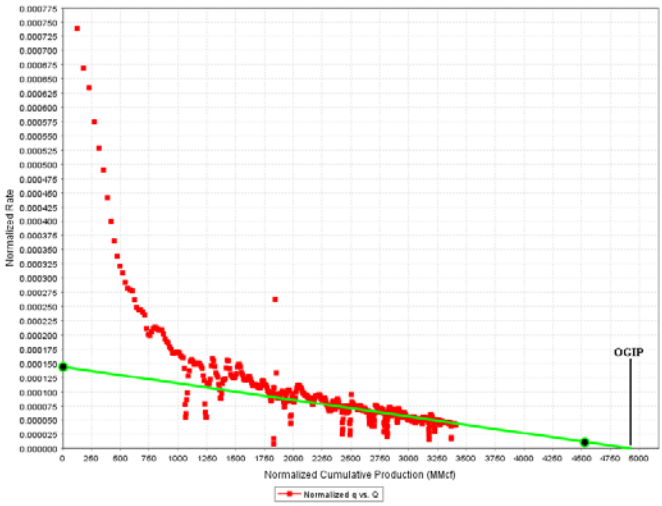


Figure 19: Noramlized Rate vs. Normalized Cum of well J7 (Case 4)

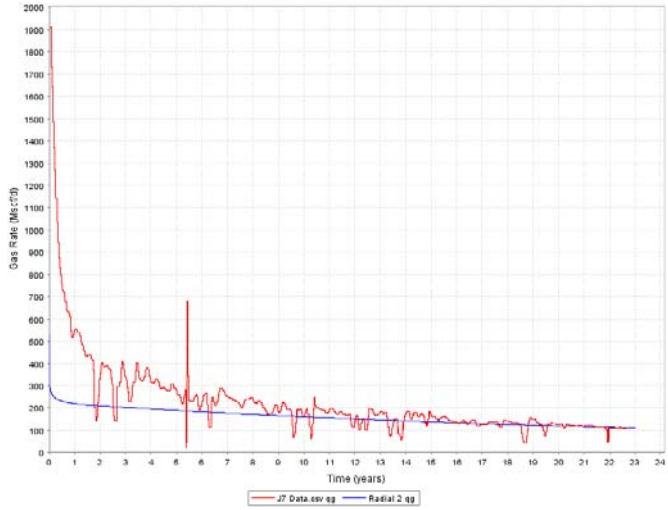


Figure 20: Raw Data and analysis of well J7 (Case 4)

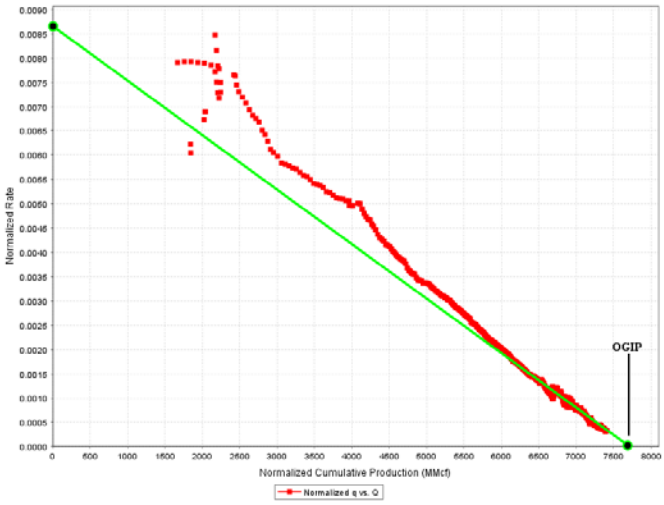


Figure 21: Normalized Rate vs. Normalized Cum. For Well HR-58 (Case 5)

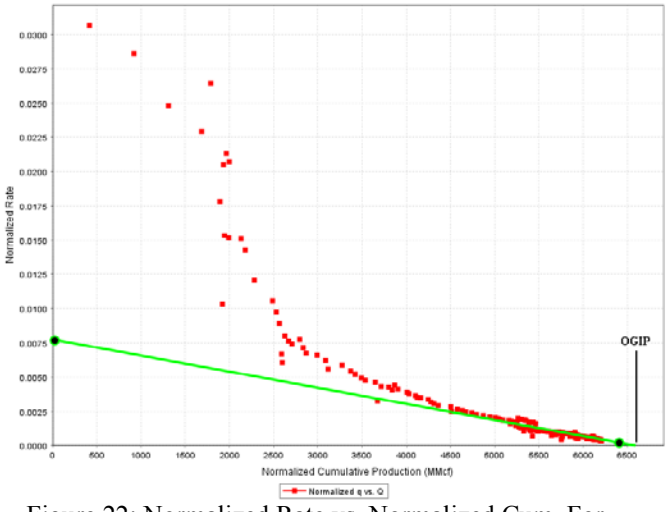


Figure 22: Normalized Rate vs. Normalized Cum. For Well HR-60 (Case 5)

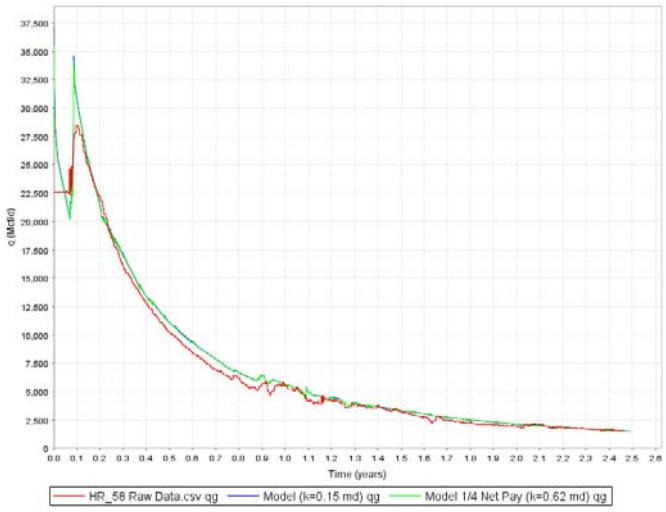


Figure 23: Raw Data and Model for well HR-58 (Case 5)


Figure 24: Raw Data and Model for well HR-58 (Case 5)

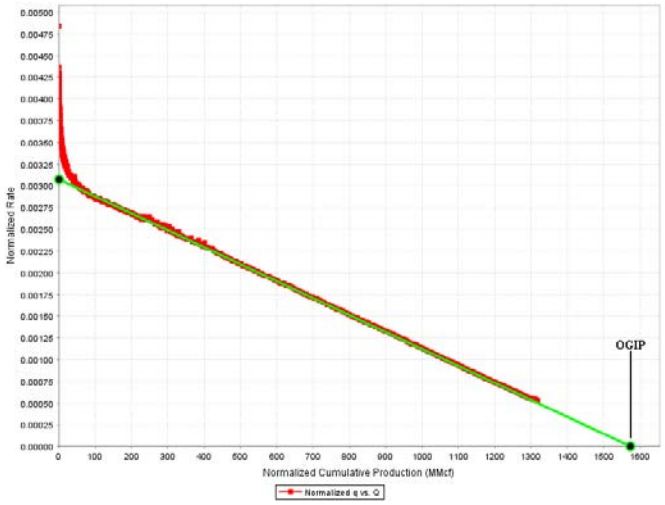


Figure 25: Normalized Rate vs Normalized Cum. Single Phase CBM (Case 6)

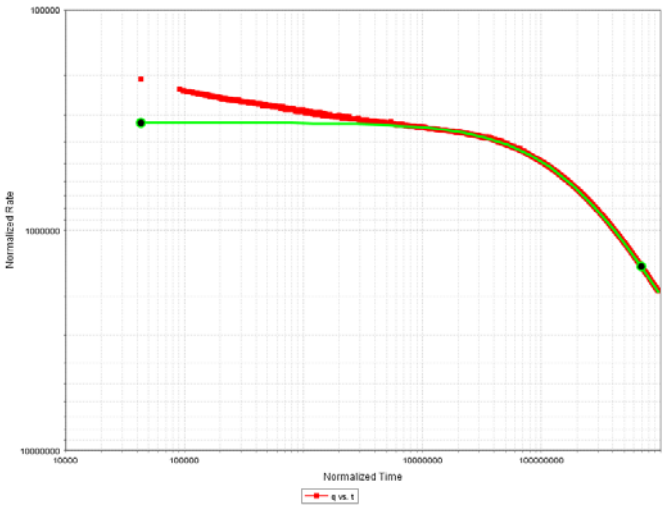


Figure 26: Normalized Rate vs. Normalized Time Single Phase CBM (Case 6)

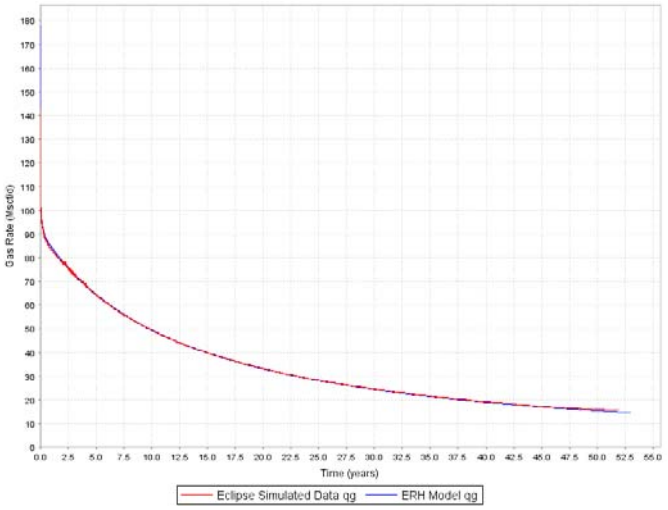


Figure 27: Simulation Data and ERH Model for Single Phase CBM (Case 6)

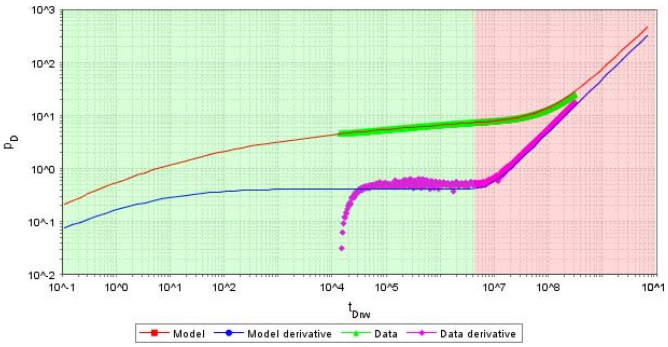


Figure 28: NPI Typecure for Single Phase CBM (Case 6)

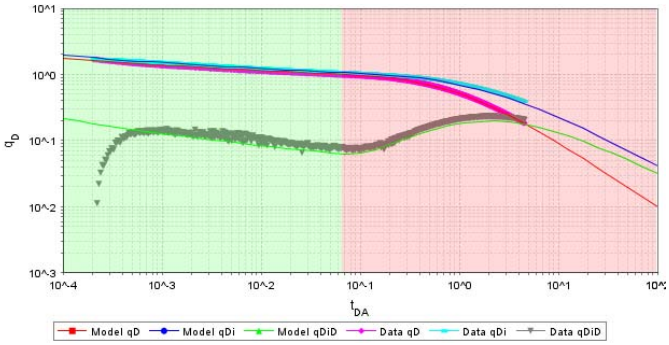


Figure 29: Blasingame Typecurve for Single Phase CBM (Case 6)

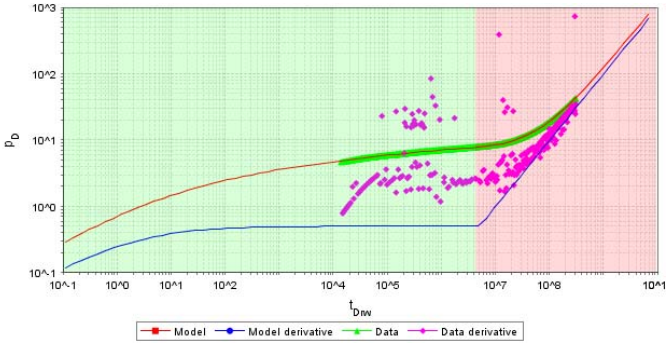


Figure 30: Bourdet Typecurve for Single Phase CBM (Case 6)

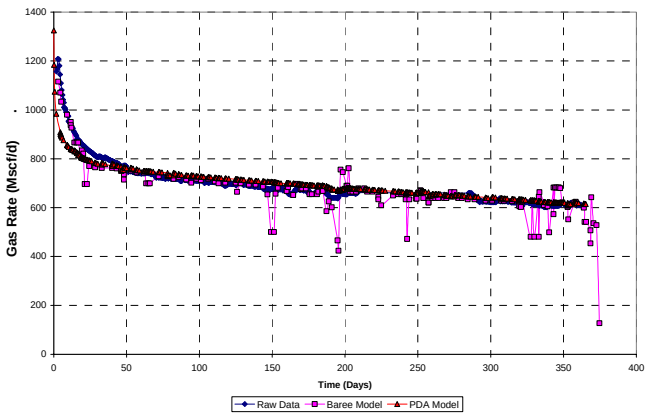


Figure 31: Raw Data and Model (Case 7)

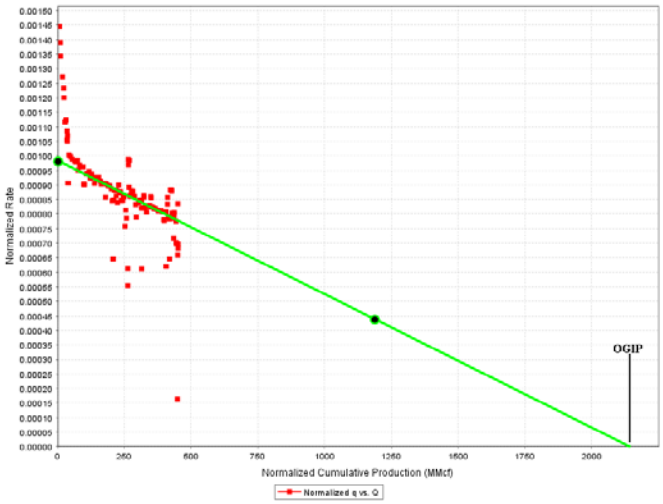


Figure 32: Normalized Rate vs. Normalized Cum. (Case 7)

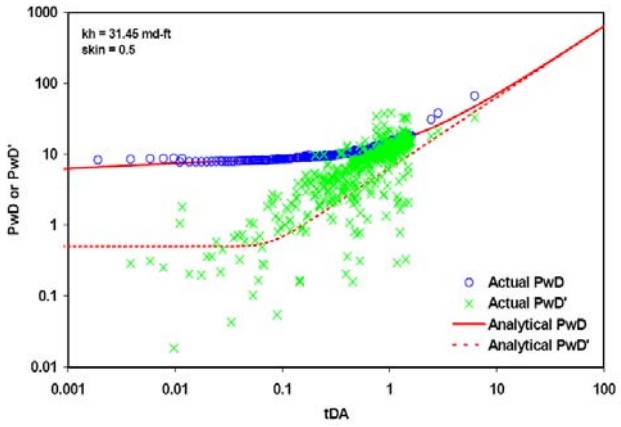


Figure 33: Baree Typecurve (Case 7)

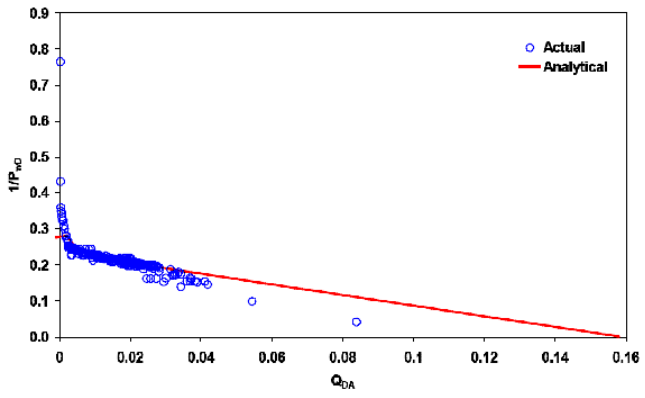


Figure 34: Barre Normalized Decline (Case 7)

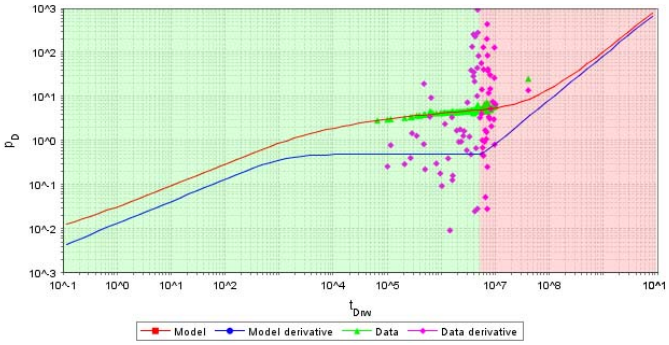


Figure 35: Bourdet Typecurve (Case 7)

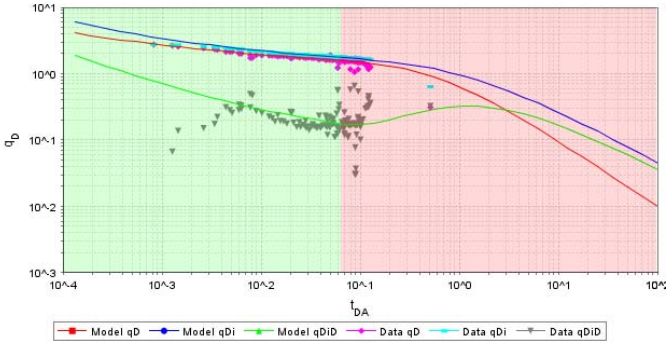


Figure 36: Blasingame Typecurve (Case 7)

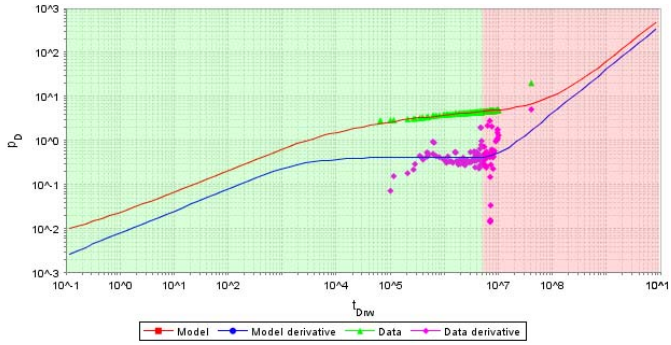


Figure 37: NPI Typecurve (Case 7)